Defence Research and
Development Canada

Recherche et développement
pour la défense Canada

DEFENCE **R&D** DÉFENSE

YBCO microbolometers for Infrared detection:

Enhancement of performances with regionally thinned microbridges

Philippe Mérel
Philips Laou
Franklin Wong
DRDC Valcartier

Canada

YBCO microbolometers for Infrared detection : **Enhancement of performances with regionally thinned microbridges**

Philippe Mérel
Philips Laou
Franklin Wong
DRDC Valcartier

Defence R&D Canada - Valcartier

Author

Philippe Mérel

Approved by

Acting Section Head

Approved for release by

Chief Scientist

Abstract

Silicon nitride microbridges (50x50 μm^2, 0.6 μm thick), suspended over a silicon substrate, were patterned and thinned. These patterns consist of 2 to 12 windows that were thinned to approximately 0.3 μm. Microbolometers were fabricated by sputtering a YBaCuO thin film over the bridges. The experimental results showed that the regionally thinned microbridges have lower thermal time constants τ (about 1.6 ms) than those of the standard pixel configurations (2.6 ms). On the other hand, the fact that these regionally thinned microbolometers having detectivity *D** values comparable to or even six times superior to those of the standard pixel showed that the decrease in response time does not result in lowered detection performance. The simulation results also show that, as the amount of material removed is increased, the thermal time constant drops significantly while the (τ / *G*)$^{1/2}$ ratio (where *G* is the thermal conductance of the pixel) only decreases slightly, suggesting that the reduced response time will not cause a significant drop in detectivity *D**. The simulation results of mechanical integrity show that a specific regionally thinned microbridge design has 22 % higher stiffness than that of a standard pixel design with similar thermal properties. The fact that thick regions remained on the regionally thinned pixels (like the edges of the pixels) provides significant mechanical support to the microstructures. This confirms the validity of the regionally thinned microbridges approach.

Résumé

Des membranes de nitrure de silicium (50x50 μm^2, épaisseur de 0,6 μm), suspendues au-dessus d'un substrat de silicium, sont amincies selon des motifs prédéterminés. Ces différents motifs sont formés de fenêtres (de 2 à 12) où la membrane est amincie pour obtenir une épaisseur finale de 0,3 μm. Des microbolomètres ont été fabriqués par pulvérisation de couches minces de YBaCuO recouvrant les membranes. Les résultats expérimentaux montrent que les membranes amincies ont une constante de temps thermique τ plus petite (environ 1,6 ms) comparativement à la configuration standard (2,6 ms). D'un autre côté, la détectivité *D** des microbolomètres amincies est comparable ou même 6 fois plus élevée que celle des microbolomètres avec une configuration standard, ceci montre que la réduction de la constante de temps thermique n'entraîne pas une baisse de la sensibilité. Les résultats de la simulation montrent qu'en amincissant les membranes, τ diminue, mais le rapport (τ / *G*)$^{1/2}$ (où *G* représente la conductance thermique du microbolomètre) baisse très peu, ce qui implique que *D** ne serait que très peu affecté. La simulation des propriétés mécaniques des membranes amincies montre une rigidité de 22% supérieure à celle d'une membrane de configuration standard avec des propriétés thermiques similaires. Cela confirme la validité de l'approche.

This page intentionally left blank.

Executive summary

Microbolometers are thermal detectors used for infrared imaging in the 8 to 12 μm spectral region. This type of infrared imager is particularly interesting since it is operated at room temperature, thus not requiring expensive and cumbersome cooling units. Microbolometers work on the principle that the temperature change caused by the absorbed radiation produces a change in the electrical resistance of the active material. This resistance variation is monitored by applying a constant current and measuring the voltage response. In order to maximize the IR response, the microbolometer needs to be thermally isolated in order for the change in temperature to be sufficient. This is done by placing the active material on suspended structures using micro-fabrication methods. Important drawbacks of thermal detectors are that they are not as sensitive or as fast as semiconducting sensors. One way to improve the sensitivity and speed of these detectors is to optimize the supporting structures of the pixels. Conventionally, the suspended structure is flat, with a uniform thickness over the entire surface. If the thickness of the structure is reduced in order to achieve higher speeds, it causes to a low mechanical integrity.

Our approach is to selectively thin out regions of the supporting structure in order to reduce material quantity while maintaining structural integrity. Using this method, it is hoped to produce thin pixels while retaining sufficient mechanical strength and measuring important characteristics like response time and detectivity. Microbolometers with regionally thinned microbridges have been produced using microfabrication techniques. The experimental results show that the regionally thinned microbridges have a lower thermal time constants than the standard pixel configuration. On the other hand, the increased speed is not accompanied by a loss of detection performance. The simulation results show that the thin pixel design, presents a higher stiffness than a comparable flat design. Also, thermal properties suggests that the increased speed will not cause a significant drop in detectivity $D*$, which is in total agreement with the experimental results.

It is shown from this work that the regionally thinned microbridge approach is a promising technology for the fabrication of fast, sensitive and robust uncooled infrared imagers.

Sommaire

Les microbolomètres sont des détecteurs thermiques utilisés pour l'imagerie infrarouge dans la gamme spectrale allant de 8 à 12 µm. Ce type d'imageur infrarouge est particulièrement intéressant puisqu'il fonctionne à la température de la pièce, ne nécessite pas d'unité de refroidissement chère et encombrante. Les microbolomètres fonctionnent selon le principe que le changement de température provoqué par l'absorption du rayonnement infrarouge entraîne un changement de résistance électrique du matériau actif. Ce changement de résistance est suivi en appliquant un courant constant et en mesurant le voltage. Afin de maximiser la réponse dans l'infrarouge, le microbolomètre doit être isolé thermiquement pour que les changements de température soient suffisamment élevés. Pour ce faire, on place le matériau actif sur une structure suspendue en utilisant des techniques de microfabrication. L'inconvénient des détecteurs thermiques est qu'ils ne sont pas aussi sensibles et rapides que les détecteurs semiconducteurs. Une façon d'améliorer la sensibilité et la rapidité est d'optimiser la structure qui supporte les pixels. De façon conventionnelle, la structure suspendue est plate, avec une épaisseur uniforme sur toute la surface. Si l'épaisseur de la structure est réduite afin d'obtenir une plus grande rapidité, cela réduit l'intégrité mécanique.

Notre approche est d'amincir de manière sélective des régions de la structure de support afin de réduire la quantité de matériel tout en maintenant l'intégrité mécanique de la structure. En utilisant cette méthode, on espère produire des pixels minces suffisamment solides pour mesurer les caractéristiques importantes comme le temps de réponse et la détectivité. Des micro-bolomètres avec des membranes amincies de façon sélective ont été produits grâce à des techniques de microfabrication. Les résultats expérimentaux montrent que ces microbolomètres ont une constante de temps plus basse que ceux de configuration normale. Ce temps de réponse plus rapide ne s'accompagne pas d'une dégradation de la détectivité. Les résultats de simulation montrent qu'un microbolomètre de conception nouvelle présente une résistance mécanique plus élevée qu'un autre microbolomètre comparable de configuration normale. Les propriétés thermiques obtenues par simulation suggèrent un temps de réponse rapide sans perte de détectivité, conformément aux résultats expérimentaux.

Il ressort de ce travail que le fait d'amincir de manière sélective des régions de la structure de support constitue une technologie prometteuse pour la fabrication d'imageurs infrarouge non refroidis rapides, sensibles et robustes.

Table of contents

List of figures

List of tables

Acknowledgements

The authors wish to acknowledge David Alain and Louis Durand for their outstanding technical support.

This page intentionally left blank.

1. Introduction

There is a constant need for improving target detection and engagement capabilities in battlefield situations. As a result, thermal or infrared (IR) imaging is becoming popular because it provides a visual capability in complete darkness and in other reduced visibility conditions.

Current thermal or IR imaging is provided by one of two main technologies: (i) photon detection mechanism and (ii) thermal detection mechanism. Photon detection is achieved when a photon detector is exposed to light radiation, resulting in direct interaction of the radiation with the atomic lattice of the material. This interaction produces parameter changes, usually in electronic form, that are detected by associated circuitry or interfaces. Different materials respond to different wavelengths of radiation and the material used to make the detector has to be electro-optically sensitive to radiations of wavelengths between 3 and 14 μm for effective night vision missions. Although photon detectors are more sensitive than thermal detectors, they operate at about 100 degrees Kelvin and below to suppress thermal noise and, as a result, cryogenic cooling is required. The cooling may be achieved using a liquid nitrogen dewar, stirling cooler, or multistage thermoelectric cooler (TEC). These add to the weight, size, and power consumption of the IR imaging systems. This is one of the major challenges to produce man-portable units or systems with this technology.

Thermal detection is achieved when the absorbed radiation changes the temperature of a thermal detector, thereby modifying its physical parameters. These physical parameters may be electrical resistance, capacitance, or mechanical displacement and can be monitored by instruments or circuitry. Although thermal detectors are less sensitive than photon detectors, thermal detectors can operate at room temperature and, therefore, compact systems can be built without cooling modules. As a result, many man-portable surveillance systems have been built using uncooled thermal technology.

Most of the uncooled thermal detector's and imager's operation is based on two principles: bolometeric and pyroelectric effects. Resistive bolometers depend on a change in the resistance of a material caused by a temperature rise when IR radiation is absorbed. Pyroelectric materials generate an external current in the absence of electrical bias by a time-dependent temperature change (e.g. the use of a mechanical chopper) caused by IR absorption. In both cases, a suspended microstructure or a microbridge is needed to thermally isolate the IR absorbing material from the substrate so as to maximize the sensitivity.

In the design of uncooled focal plane arrays, many parameters govern the performance like overall mass and leg length. For example, when designing microbolometers, it is sometimes desired to use thin microbridges in order to reduce the response time, thus providing faster response. The faster response time comes from a reduction in thermal mass of the microbolometers. However, by using thin microbridges, there is a risk of reducing the mechanical strength of the pixels, leading to less robust imaging systems. Our objective is to produce thin pixels while retaining sufficient mechanical strength and measuring important characteristics like response time and detectivity. We propose a scheme of regional thinning

of the microbridges. Using this method, windows on the microbridges will be thinner than the edges, as illustrated in Figure 1. These thicker edges will act as supporting structures.

Thinning the microbridges will also affect the sensitivity and the detectivity of the microbolometers. Indeed, thin microbridges have smaller thermal time constant (τ) due to the reduction in overall mass. They also present a lower thermal conductance (G) since the cross-section of the microbridge is reduced, thus decreasing the heat flow from the center of the microbridge towards the substrate through the supporting legs. Since the signal-to-thermal noise ratio of microbolometers is proportional to the $(\tau / G)^{1/2}$, it is important to optimize this value by choosing the appropriate microbridge design.

The purpose of this work is to study the optical and mechanical properties of different designs of regionally thinned microbolometers through experimental work and simulation. The experimental and simulation results are presented.

This work was supported under Work Breakdown Element 12pa12 (formerly 12kc12) entitled "Autonomous Micro Sensors". The information contained in this document describes the work performed on the project at DRDC Valcartier between March and September 2004.

50 μm

Figure 1. *Different designs of regionally thinned microbolometers having 2, 3, 4, 6, 8 and 12 windows. The light gray regions are thinner than the dark gray regions.*

2.   Experimental procedure

In this work, six different regionally thinned microbolometer designs were evaluated and compared to the performance of the standard pixels. The different microbolometer designs are presented in Figure 1 and Table 1 presents the width (in μm) of the different windows, the overall width of the pixel is 50 μm in all cases. Each sample consists of a total of 48 pixels, including four pixels of each design and 24 standard pixels. By having all the pixels on the same sample, one can compare their performances without the possible effect of different processing conditions.

Table 1. Windows dimensions

| Number of windows on microbridge	Width of windows (μm)
2	22
3	14
4	10
6	6
8	4
12	2

Microfabrication techniques were used to produce the microbolometers[2]. A 0.6 μm thick silicon nitride (Si_3N_4) thin film was deposited by chemical vapor deposition (CVD) on a silicon substrate. The microbridges were first defined using UV lithography and the silicon nitride thin film was then etched using reactive plasma etching (RIE) in a $He/CHF_3/SF_6$ gas mixture. In a second lithography step, the windows on the pixel were defined and the thickness of the window regions was reduced to 0.3 μm. The Si_3N_4 membranes were then released by chemical etching of the silicon substrate using KOH solution at 70 °C. A 0.1 μm thick YBCO thin film was then sputtered on the microbridges by RF magnetron sputtering with the following conditions: Ar pressure of 3 mTorr, RF power of 40 W and a deposition time of 4 hours. This material is the active component of the device. Since its resistivity changes as temperature changes, the incident radiation to the YBCO film can be measured by monitoring the change of resistance as the YBCO film and the underlying Si_3N_4 microbridge are exposed to infrared radiation. A 0.15 μm Au thin film is deposited on top of the YBCO thin film also using RF magnetron sputtering. This final layer is used as an electrical conductor. Two lithography steps combined with chemical etching of the YBCO and Au thin films complete the microbolometer fabrication. The resulting microbolometers have resistance values ranging from 0.2 to 2 MΩ. Figure 2 presents a scanning electron microscope (SEM) image of a pixel having four windows.

The sensitivity (*S*) and the detectivity (*D**) of the microbolometers were measured at different bias currents. A glow bar was used as the infrared source. A chopper ($f = 10$ Hz) was used to modulate the power on the microbolometers and the voltage modulation was measured using

a lock-in amplifier. The percentage change in resistance with temperature (*TCR*) of the microbolometers was measured from 285 to 315 K. τ was evaluated by measuring the sensitivity as a function of frequency using the following equation[3]:

$$S = R\eta(TCR)I/G(1+w^2\tau^2)^{1/2}$$ Equation 1.

Where *R* is the resistance of the microbolometer, η is the absorption coefficient, *I* is the bias current, *G* the thermal conductance, and *w* the modulation of angular frequency of the incident radiation.
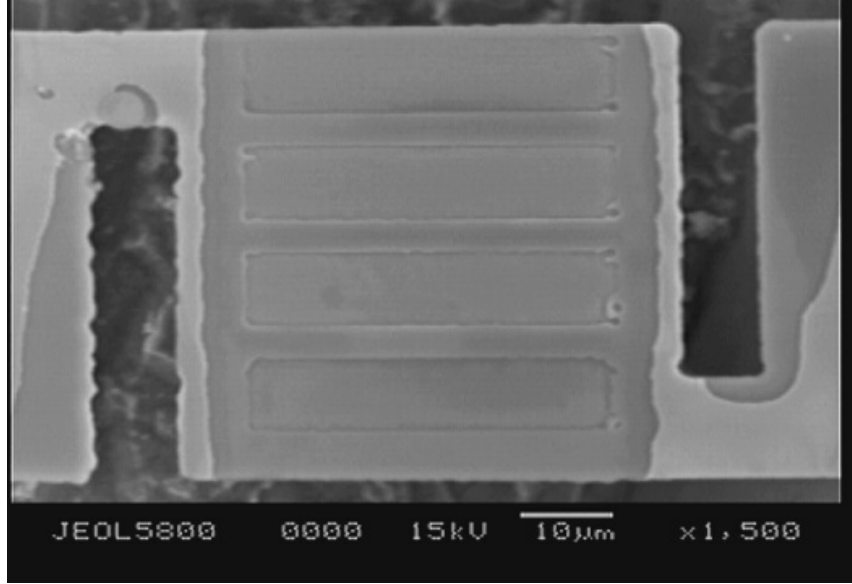
Figure 2. *SEM image of a regionally thinned microbolometer having four windows.*

DRDC Valcartier TM 2006-496

3.   Experimental results

Table II presents τ and G of a standard pixel and three designs of regionally thinned microbolometers having 3, 6 and 12 windows. As expected, and for all the thin pixel designs, τ was reduced by about a factor of 1.6 compared to the standard pixel. However, the different values of G do not present a clear result. These values could be affected by processing issues related to the gold coverage of the microbolometers.

Table 2. Thermal time constant and thermal conduction of regionally thinned microbolometers

Microbolometer design	Thermal time constant τ (ms)	Thermal conductance G (μW/K)
Standard pixel	2.6	2.1
3 windows	1.7	2.3
6 windows	1.6	4.6
12 windows	1.5	3.0

From the results presented in Table II, it is clear that the regional thinning of the microbridges reduces, as expected, the time response of the microbolometers. But it is also important to know the impact on detectivity of these designs. Figure 3 presents the detectivity of standard and regionally thinned microbolometers (except for the 3 and 12 windows because of process problems) as a function of bias current with a modulation frequency (f) of 10 Hz. It is first observed that the two standard pixels (#5 and #29) have a very similar detectivity at around 5×10^6 cm-Hz$^{1/2}$/W. This value will serve as a baseline for comparison purposes. The two and four window designs show a detectivity about a factor of two higher than that of the standard pixels at about 1×10^7 cm-Hz$^{1/2}$/W. The six window design presents the highest detectivity at about 3×10^7 cm-Hz$^{1/2}$/W. Only the eight window design shows a lower D^* than that of the standard pixels at about 2.5×10^6 cm-Hz$^{1/2}$/W. Variations in D^* values can also be partly caused by differences in thin film thickness and supporting leg widths. For future work, better uniformity in processing conditions would reduce these variations.

These results show that, at $f = 10$ Hz, the detectivity is maintained or increased for regionally thinned microbridges compared to the standard pixels. However, at this low frequency, the biggest D^* limitation might be $1/f$ noise. Johnson noise is also limiting D^*, not just the thermal noise.

Also, the *TCR* values of the different microbolometers were measured to be uniform at about –2.5 %/K.
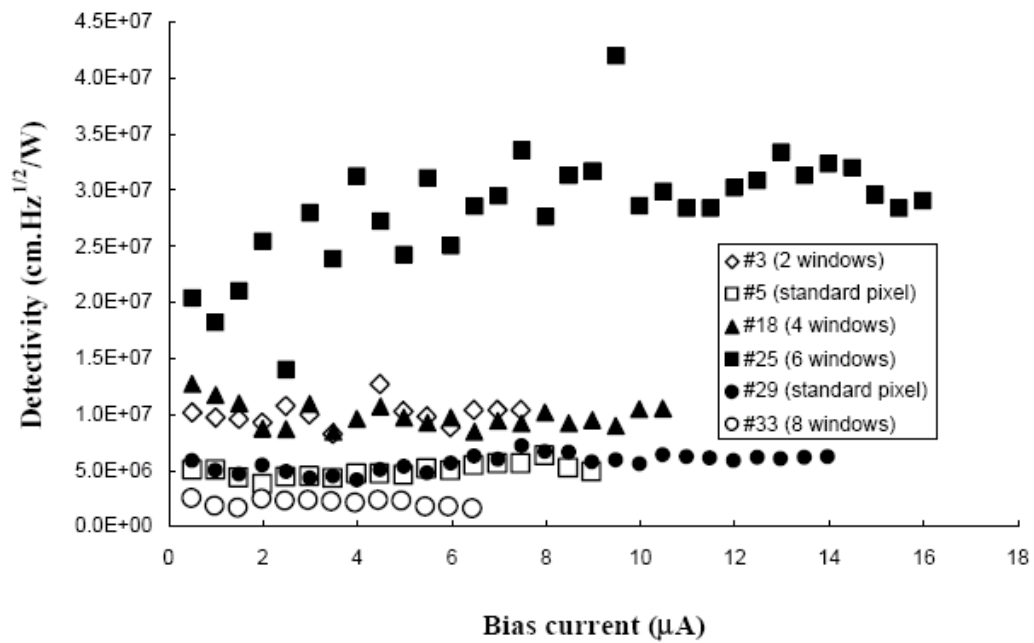
Figure 3.*: Detectivity of regionally thinned microbolometers as a function of bias current (f = 10 Hz).*

4.   Parametric finite element study

In order to understand the impact of the microbridge structure on the mechanical and thermal properties of the resulting microbolometer, a finite element model was constructed with 8-noded iso-parametric hexahedral elements to capture the three-dimensional features of the thinned sections in the pixel area. The thermal element had a single degree of freedom, temperature, at each node. The structural element had three degrees of freedom, x, y and z displacement, at each node. The micron-kilogram-second units were used in place of the standard metre-kilogram-second units to accommodate the micron-based geometry. Therefore, pressure is expressed in mega-pascals (MPa), heat flux is in terms of pico-Watts (pW) and energy has the units pico-Joules (pJ).

The idealized thickness distribution of the Si_3N_4, YBCO and Au layers for the standard bolometer configuration are given in Table III. Compared to the pixel area linear dimensions (50 μm × 50 μm), the aspect ratio of area length (l) to layer thickness (t) varies between 167 < l/t < 500. A mesh sensitivity study was carried out to determine a suitable aspect ratio that would minimize the structural and thermal elemental energy error norms. We found that each layer had to be at least two element thick to capture the bending stresses from pressure loading. The error norm increased as the l/t ratio increased as expected. To achieve a reasonable energy norm of less than 0.1 and to stay within the memory capacity of our computer, the surface area dimensions of an element were selected to be 0.5 μm × 0.5 μm thereby giving aspect ratios ranging from 3.3 < l/t < 10. Figure 4 is a close-up view of the bolometer solid model before meshing. A thinner bolometer configuration without a layer 3 and 4 was also included. The dimensions for this configuration are given in Table IV. The material properties used in this study are given in Table V.

Table 3. Idealized thickness distribution of bolometer materials for standard configuration

Layer	Material	Thickness (μm)	Cumulative Thickness (μm)
6	Au	0.15	0.85
5	YBCO	0.1	0.7
4	Si_3N_4	0.2	0.6
3	Si_3N_4/YBCO	0.1	0.4
2	Si_3N_4	0.3	0.3
1	--	--	0

Table 4. Idealized thickness distribution of bolometer materials for thin configuration

Layer	Material	Thickness (μm)	Cumulative Thickness (μm)
6	Au	0.15	0.694
5	YBCO	0.1	0.544
4	Si_3N_4	0.444	0.444
1	--	--	0

Table 5. *Material properties*

Property	Si$_3$N$_4$	YBCO[a]	Au	References.
Modulus (MPa)	310×10^3	310×10^3	77.2×10^3	6
Poisson ratio (--)	0.27	0.27	0.42	6
Density (kg/μm^3)	3290×10^{-18}	3290×10^{-18}	19320×10^{-18}	6
Thermal Expansion (K^{-1})	3.3×10^{-6}	3.3×10^{-6}	14.4×10^{-6}	6
Specific heat (pJ/kg-K)	680×10^{12}	544×10^{12}	132.3×10^{12}	6
Thermal conductivity (pW/μm-K)	30×10^6	10×10^6	301×10^6	6, 7

[a] YBCO mechanical properties assumed equal to Si$_3$N$_4$ properties

A comparative approach was employed for the finite element study because actual structural and thermal loading conditions were not available. The structural load was defined as a surface pressure that arises from processing operations. A nominal value of 0.01 MPa was used in the calculations. The free ends of the microbridge's arms were fully constrained from moving. For thermal loading, a heat flux of 1640 pW/μm^2 was selected. This value was based on experimental measurements. The temperature at the free ends of the micro-bride's arms was fixed at 0 K.

Figure 4 shows the regions where results were taken. Structural performance will be evaluated along Line 1 and Line 2. Thermal performance will be compared with results taken along Line 3. Baseline results are calculated from a standard pixel.
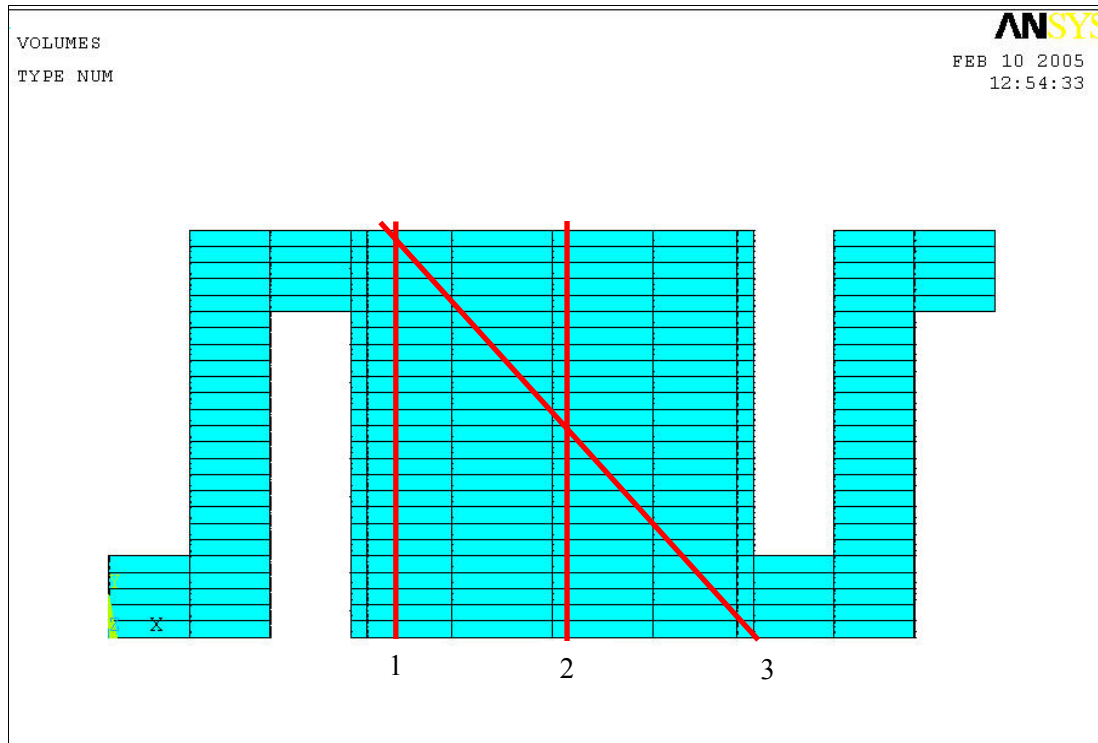
**Figure 4.** *Identification of regions used for data reduction.*

Figure 5 shows how the microbolometer generally deforms under pressure loading. The structural impact of thinning the active pixel area is shown in Figures 6 and 7. Generally, the more the pixel deforms under pressure, the higher the stresses and strains in the material. Along the edge of the pixel (see Figure 6), deformation increases from where the bolometer arms are attached to the pixel. The reductions in stiffness as compared to the baseline pixel are 18 %, 35 % and 39 % for the 12 (ST-02MU), 3 (ST-14MU) and 2 (ST-22MU) windows designs, respectively. The relative loss in stiffness between 3 and 2 windows is much less than the relative loss in stiffness between 12 and 3 windows designs. Because there are no trenches, the thinned pixel without any windows (ST-00TH) is more flexible than the 12 window configuration (22%). Along the pixel centerline (see Figure 7), the 12 and 3 window configurations experience similar reductions in stiffness at y = 0 as found in the edge results. The loss in Si_3N_4 for 2 windows has a larger effect on the centerline deflections. The thinned pixel is more deformed than the 12 window configuration in the center as well.

Figure 8 shows the temperature contours at steady state conditions under a uniform heat flux. Using this information, relative values for τ, G and the ratio $(\tau / G)^{1/2}$ for different microbolometer configurations were evaluated. This information is presented in Table VI. The first observation is that the standard pixel with a thickness of 0.444 μm and the 12 window configuration have very similar thermal characteristics. For these two cases, the $(\tau / G)^{1/2}$ ratio, which is proportional to the signal-to-thermal noise ratio, is higher than that of the standard pixel with a thickness of 0.6 μm. As the amount of material removed is increased (the 3 and 2 window cases), the thermal time constant drops significantly. This increased

speed is accompanied by a modest drop of the $(\tau / G)^{1/2}$ ratio, suggesting that the reduced response time will not cause a significant drop in detectivity D^*. This confirms the experimental results presented in Table 2 and Figure 3 where regionally thinned micro-bolometers having shorter time constants do not show a reduction in detectivity. The absorption coefficient η was assumed to be constant for all pixel types. Variations in η should be considered in future work.
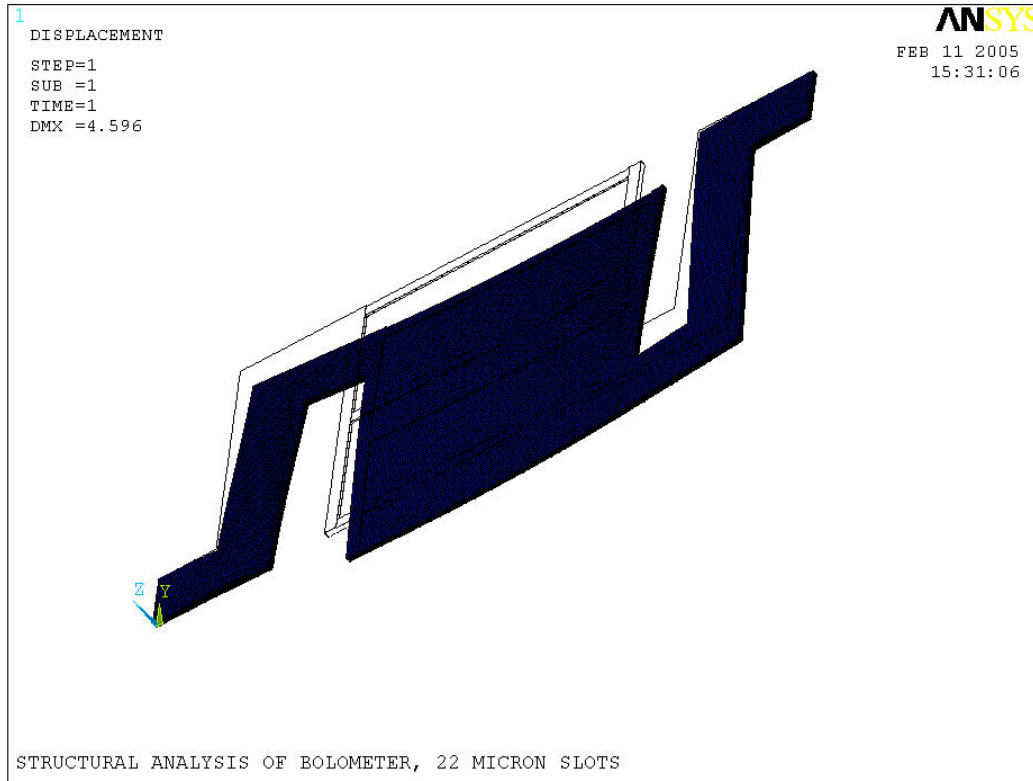
Figure 5. General bolometer deformation under pressure loading
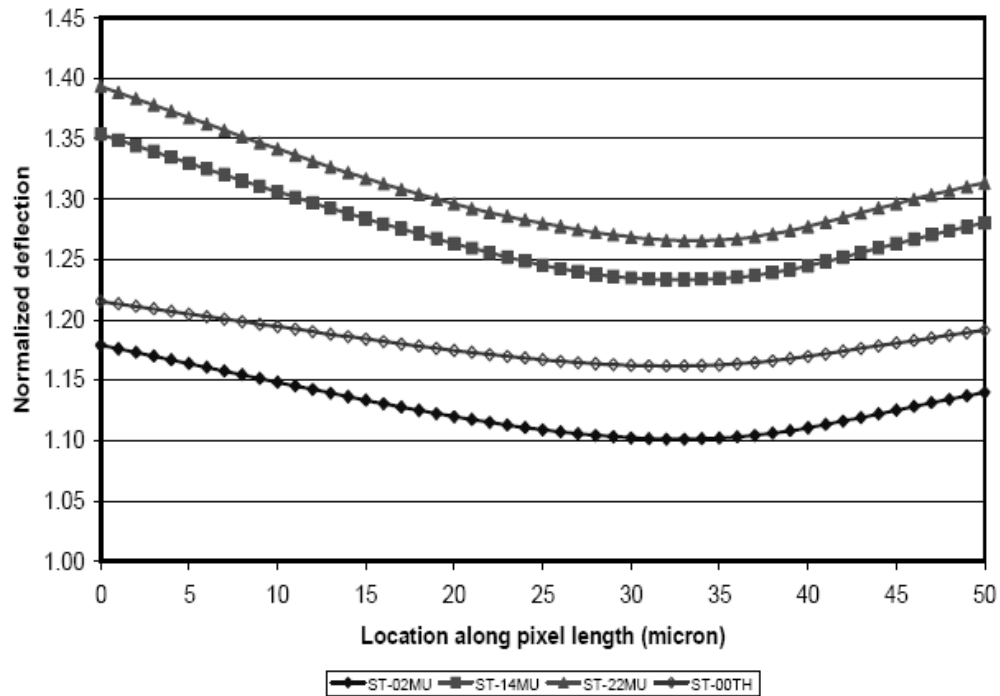
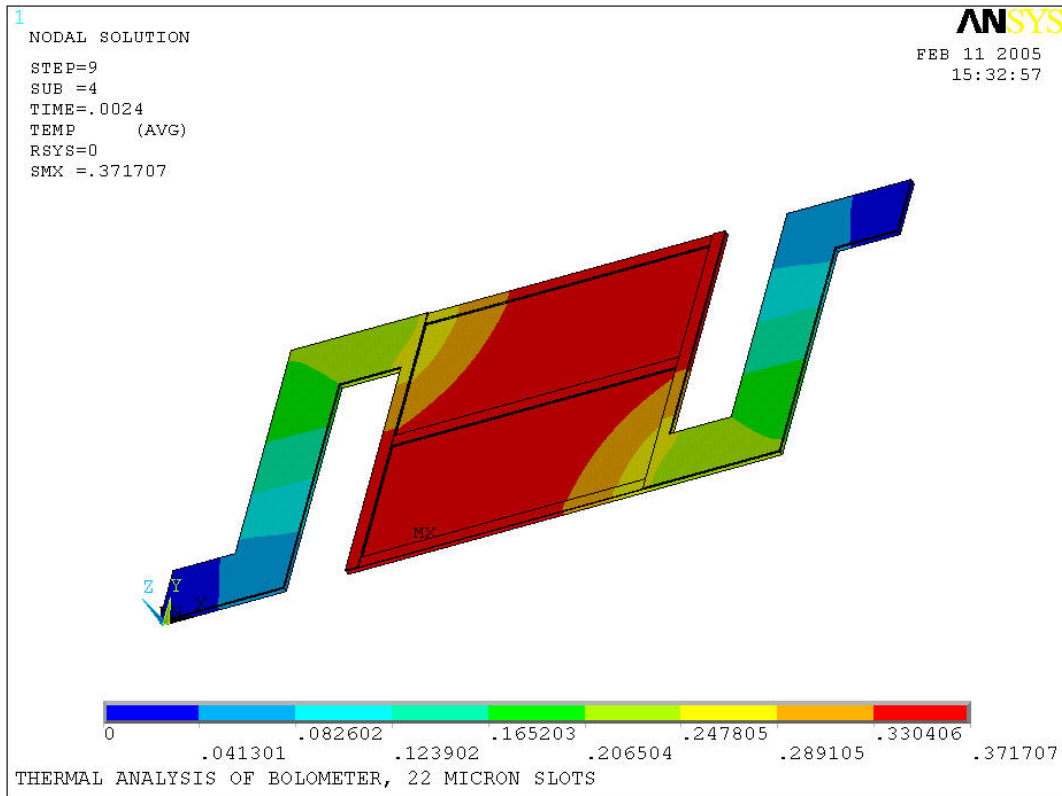***Figure 6.*** *Vertical (z) deflection of pixel surface along edge (Line 1) where location 0 μm corresponds to y = 0.*
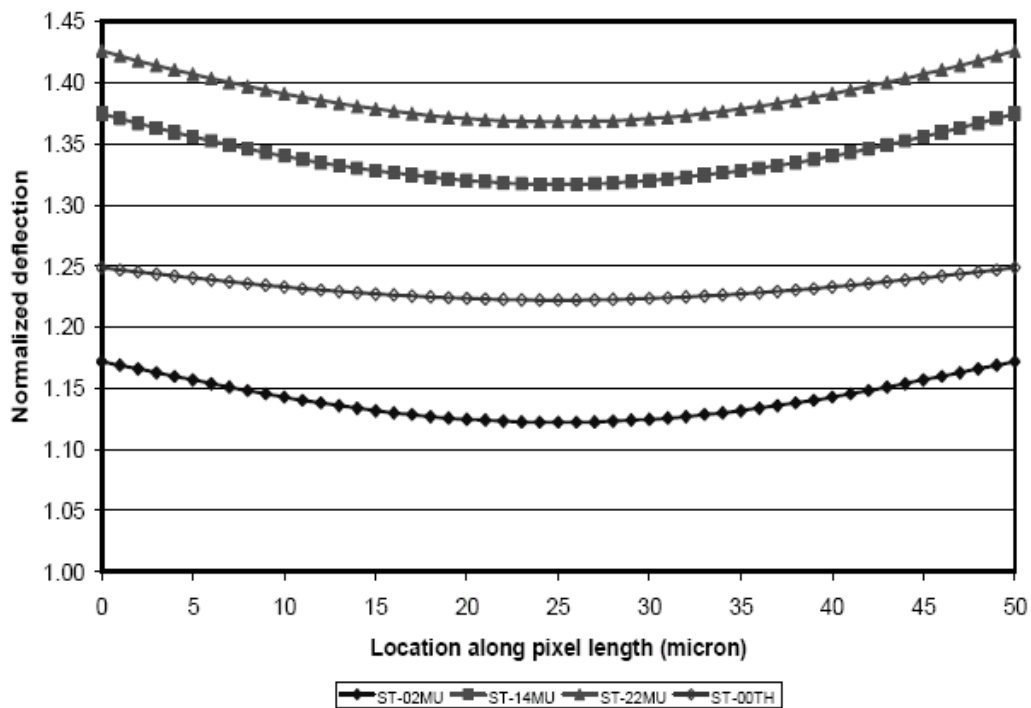
Figure 7. *Vertical (z) deflection of pixel surface along center (Line 2) where location 0 μm corresponds to y = 0.*

Figure 8. Temperature distribution at steady state conditions from uniform heat flux

Table 6. Simulated values for the thermal time constant and the thermal conduction of regionally thinned microbolometers compared with a standard pixel.

Microbolometer design	τ (a.u.)	G (a.u.)	$(\tau/G)^{1/2}$ (a.u.)
Standard pixel (thickness of 0.6 μm)	1	1	1
Standard pixel (thickness of 0.444 μm) (ST-00TH)	1	0.94	1.03
12 windows (ST-02MU)	1	0.94	1.03
3 windows (ST-14MU)	0.87	0.91	0.98
2 windows (ST-22MU)	0.87	0.90	0.98

5. Conclusions

Our objective was to produce thin pixels while retaining sufficient mechanical strength and measuring important characteristics like response time and detectivity. Microbolometers with regionally thinned microbridges have been produced using micro-fabrication techniques. The experimental results show that the regionally thinned microbridges have a lower thermal time constants (about 1.6 ms) than the standard pixel configuration (2.6 ms). On the other hand, the regionally thinned microbolometers show $D*$ values comparable or even six times superior to that of the standard pixel. This implies that the increased speed is not accompanied by a loss of detection performance.

The simulation results show that the 12 window design, which has the same thermal properties as the 0.444 μm thick standard pixel, will have a 22 % higher stiffness. This confirms the validity of the regionally thinned microbridges approach. Also, as the amount of material removed is increased, the thermal time constant drops significantly while the $(\tau/G)^{1/2}$ ratio only decreases slightly, suggesting that the increased speed will not cause a significant drop in detectivity $D*$, in total agreement with the experimental results.

6.   References

1. S. Horn, J. Campbell, P. Perconti, D. Lorhmann, Uncooled IR Technology and Applications, TTCP-SEN TP4, 2002.

2. P. Laou, L. Ngo Phong, "Effects of Bridge pattern on performance of YBaCuO microbolometers", J. Vac. Sci. Technol. A **20**, 1659 (2002).

3. E. L. Dereniak, G. D. Boreman, Infrared Detectors and Systems, John Wiley and Sons, New York, 1996.

4. ANSYS Release 8.0 (2003), Coupled Field Analysis Guide, Sec. 1.3 System of Units

5. Zienkewicz, O., Zhu, J.Z., "A Simple Error Estimator and Adaptive Procedure for Practical Engineering Analysis", Int. J. for Numerical Methods in Engineering **24**, 337 (1987).

6. MatWeb.com, www.matweb.com/search/SpecificMaterialPrint.asp?bassnum=meau00, 16 Dec. 2004

7. NIST WEBHTS Database, http://www.ceramics.nist.gov/srd/hts/htsquery.htm, 08 February 2001.

List of symbols/abbreviations/acronyms/initialisms

DND	Department of National Defence
τ	Thermal time constant
G	Thermal conductance of microbridges
S	Sensitivity of microbolometers
D*	Detectivity of microbolometers
f	Chopper frequency
TCR	Percentage change in resistance with temperature
R	Resistance of microbolometer
η	IR absorption coefficient
I	Bias current
w	Modulation of angular frequency of the incident radiation
l	Length of microbolometer
t	Layer thickness

Glossary

Technical term	Explanation of term
Microbolometer	Infrared detector (typically having dimensions of 50 x 50 μm^2). The working principle is that the temperature change caused by the absorbed radiation produces a change in the electrical resistance of the active material.
Detectivity	A parameter used to compare the performance of different detector types. $D*$ is the signal-to-noise ratio at a particular electrical frequency and in a 1 Hz bandwidth when 1 Watt of radiant power is incident on a 1 cm^2 active area detector. The higher $D*$ the better the detector.

Distribution list

INTERNAL DISTRIBUTION

1 – Director General

1 – Head / TSR

1 – Head / PW

3 – Document Library

1 – P. Mérel (author)

1 – P. Laou (author)

1 – F. Wong (author)

EXTERNAL DISTRIBUTION

1 _ Library and Archives Canada

1 – DRDKIM (PDF file)

1 – DRDC

FICHE DE CONTRÔLE DU DOCUMENT

1. PROVENANCE (le nom et l'adresse) DRDC Valcartier, 2459, boul. Pie-XI nord, Québec (Québec) G3J 1X5	2. COTE DE SÉCURITÉ (y compris les notices d'avertissement, s'il y a lieu) sans classification

3. TITRE (Indiquer la cote de sécurité au moyen de l'abréviation (S, C, R ou U) mise entre parenthèses, immédiatement après le titre.)

YBCO microbolometers for infrared detection: enhancement of performances with regionally thinned microbridges

4. AUTEURS (Nom de famille, prénom et initiales. Indiquer les grades militaires, ex.: Bleau, Maj. Louis E.)

Mérel, Philippe, PM; Laou, Philips, PL; Wong, Franklin, FW

5. DATE DE PUBLICATION DU DOCUMENT (mois et année) June 2009	6a. NOMBRE DE PAGES 27	6b. NOMBRE DE REFERENCES 7

7. DESCRIPTION DU DOCUMENT (La catégorie du document, par exemple rapport, note technique ou mémorandum. Indiquer les dates lorsque le rapport couvre une période définie.)

mémorandum

8. PARRAIN (le nom et l'adresse)

9a. NUMÉRO DU PROJET OU DE LA SUBVENTION (Spécifier si c'est un projet ou une subvention)	9b. NUMÉRO DE CONTRAT
10a. NUMÉRO DU DOCUMENT DE L'ORGANISME EXPÉDITEUR	10b. AUTRES NUMÉROS DU DOCUMENT N/A

11. ACCÈS AU DOCUMENT (Toutes les restrictions concernant une diffusion plus ample du document, autres que celles inhérentes à la cote de sécurité.)

☒ Diffusion illimitée
☐ Diffusion limitée aux entrepreneurs des pays suivants (spécifier)
☐ Diffusion limitée aux entrepreneurs canadiens (avec une justification)
☐ Diffusion limitée aux organismes gouvernementaux (avec une justification)
☐ Diffusion limitée aux ministères de la Défense
☐ Autres

12. ANNONCE DU DOCUMENT (Toutes les restrictions à l'annonce bibliographique de ce document. Cela correspond, en principe, aux données d'accès au document (11). Lorsqu'une diffusion supplémentaire (à d'autres organismes que ceux précisés à la case 11) est possible, on pourra élargir le cercle de diffusion de l'annonce.)

Illmitée

dcd03f ver.(06-1999)

13. SOMMAIRE (Un résumé clair et concis du document. Les renseignements peuvent aussi figurer ailleurs dans le document. Il est souhaitable que le sommaire des documents classifiés soit non classifié. Il faut inscrire au commencement de chaque paragraphe du sommaire la cote de sécurité applicable aux renseignements qui s'y trouvent, à moins que le document lui-même soit non classifié. Se servir des lettres suivantes: (S), (C), (R) ou (U). Il n'est pas nécessaire de fournir ici des sommaires dans les deux langues officielles à moins que le document soit bilingue.)

Des membranes de nitrure de silicium (50x50 µm2, épaisseur de 0,6 µm), suspendues au-dessus d'un substrat de silicium, sont amincies selon des motifs prédéterminés. Ces différents motifs sont formés de fenêtres (de 2 à 12) où la membrane est amincie pour obtenir une épaisseur finale de 0,3 µm. Des microbolomètres ont été fabriqués par pulvérisation de couches minces de YBaCuO recouvrant les membranes. Les résultats expérimentaux montrent que les membranes amincies ont une constante de temps thermique τ plus petite (environ 1,6 ms) comparativement à la configuration standard (2,6 ms). D'un autre côté, la détectivité D* des microbolomètres amincies est comparable ou même 6 fois plus élevée que celle des microbolomètres avec une configuration standard, ceci montre que la réduction de la constante de temps thermique n'entraîne pas une baisse de la sensibilité. Les résultats de la simulation montrent qu'en amincissant les membranes, τ diminue, mais le rapport $(\tau / G)1/2$ (où G représente la conductance thermique du microbolomètre) baisse très peu, ce qui implique que D* ne serait que très peu affecté. La simulation des propriétés mécaniques des membranes amincies montre une rigidité de 22% supérieure à celle d'une membrane de configuration standard avec des propriétés thermiques similaires. Cela confirme la validité de l'approche.

14. MOTS-CLÉS, DESCRIPTEURS OU RENSEIGNEMENTS SPÉCIAUX (Expressions ou mots significatifs du point de vue technique, qui caractérisent un document et peuvent aider à le cataloguer. Il faut choisir des termes qui n'exigent pas de cote de sécurité. Des renseignements tels que le modèle de l'équipement, la marque de fabrique, le nom de code du projet militaire, la situation géographique, peuvent servir de mots-clés. Si possible, on doit choisir des mots-clés d'un thésaurus, par exemple le "Thesaurus of Engineering and Scientific Terms (TESTS)". Nommer ce thésaurus. Si l'on ne peut pas trouver de termes non classifiés, il faut indiquer la classification de chaque terme comme on le fait avec le titre.)

microbolomètre, détecteur, infrarouge,

dcd03f ver.(06-1999)

Defence R&D Canada

Canada's Leader in Defence
and National Security
Science and Technology

R & D pour la défense Canada

Chef de file au Canada en matière
de science et de technologie pour
la défense et la sécurité nationale

DEFENCE **R** **D** DÉFENSE